We thank two anonymous reviewers for their suggestions that have led to a number of minor to critical improvements. Both reviewers noted that the scientific concept of the original manuscript is good in general and the connection between melt and subglacial discharge is striking.

We are grateful to reviewer 1 for the minor comments. Reviewer 1 felt "Authors present exciting findings with a few minor corrections needed before publication." We've addressed all the concerns from reviewer 1.

We appreciate reviewer 2's suggestions to expand Section 2.2 Bathymetric Inversion Approach. Reviewer 2 felt "Given that 2D modeling underpins the inversion approach this section should be expanded." Therefore, we have added new paragraphs and figures accordingly. The main updates are:

- More details about the bathymetry processing including how the polygon densities are chosen, how the bathymetry grid was merged, and description of the final bathymetric grid.
- New paragraphs on sediment uncertainty.
- New 2D gravity model profiles included as supplementary figures (Fig. S4).
- Free-air gravity field added to Figure 2c of the main text.
- Gravity anomaly (Fig. S1) in a shaded relief view.
- Coastlines of islands added to most of the maps.

We feel that the changes we made in response to the reviewers' comments have strengthened the paper and made the manuscript more readable. We hope that we have satisfactorily responded to all comments, which can be found here below. The original reviewer comments appear in *blue italics* and our response is provided in upright black text. Where line numbers are given, they refer to the version of the manuscript with changes marked on.

RC1: Anonymous Referee #1:

General comments:

The authors showed the results of bathymetry under Getz with ice shelf draft. They also confirm the importance of subglacial discharge for controlling basal melt rate. Authors present exciting findings with a few minor corrections needed before publication.

Thank you. Please find below a few minor corrections.

Minor comment:

Why ice shelf draft is not shown? I would like to see ice shelf draft plotted in Figure 2 as well. I believe the additional discussion on the difference between previous and new dataset would be great.

The ice shelf draft is shown in the original Figure 2b. The black dots in the Figure 2b indicates ice shelf draft deeper than 500 m. The discussion on the difference between previous and new dataset can be found from Line 220, which states "The major troughs we report are not present in the publicly available Bedmap2 (Fretwell et al., 2013) or IBCSO (International Bathymetric Chart of the Southern Ocean) (Arndt 185 et al., 2013) and the bathymetric sill we observe is not represented in RTOPO2 (Schaffer and Timmermann, 2016)."

Other comments:

Line 110: Is this anomaly? Authors should phrase this better as in the caption of Figure 3.

The passage in question previously stated "Fig. 3 shows melt rate **anomalies** after the first-order influence of ocean temperature on melt has been removed." Our use of the word anomalies was incorrect. We have revised the text, which now states "Fig. 3 shows melt rate **residuals** after the first-order influence of ocean temperature on melt has been removed."

Line 127-132: Authors mention that they use the least square method to infer 3.8m /yr /K. What is this value? It would be good if authors can clarify which value they try to calculate. It would be good to add an equation in the text and specify.

Both reviewers identified that the paragraph which was previously on lines 127-132 was problematic. Our original intent was to include this somewhat superfluous paragraph as a means of adding extra clarity about our process, but after considering the reviewers' feedback we see that the entire paragraph was confusing, unnecessary, and a distraction from the description of the analysis. Thus, we have removed the problematic paragraph in this revised version of the manuscript.

By removing this paragraph, we no longer mention the confusing 3.8 m/yr/K $d\dot{m}/dT$ slope that was used to detrend the melt rate relative to basal temperature, but we note that this value is inconsequential to our findings. The detrending step was performed only for visual context, to help unmask second-order processes that are not directly related to the first-order effects of basal temperature. An error in the value we determined would merely result in shifting the average color of melt anomalies in Figure 3, but the pattern would remain the same. Thus, we agree with the reviewers that the value of 3.8 m/yr/K was confusing and needed attention, but we feel that adding more figures or equations to describe least-squares fitting would likely be more confusing and more of a distraction to readers.

The caption of Figure 2: I believe you do not mark only 500 m. What is the range?

We marked ice bottom elevation deeper than 500 m. We have revised the caption of Figure 2b as "(b) The observed basal melt rate. Black stippling indicates ice bottom elevations deeper than 500 m."

Line 154 and some other lines: Authors can not say this is Meltrate with no discharge. This is confusing. What authors did is to remove the effect of ocean temperature.

As reviewer 2 suggested, we have added a clearer definition of "melt rate with no sub-glacial discharge" up front in the corresponding method section where has the first introduction of this term. It says "We modeled the melt rates over Getz that are expected to result from the in situ farfield ocean temperature. We refer to this modeled melt rate as non-discharge melt rate through this paper since it does not consider any potential impact from local subglacial discharge." Besides, we have changed the subheading from "melt rate with no discharge" to "melt rate with no sub-glacial discharge".

Acknowledgment: I believe authors should mention where these datasets can be downloaded. Raw data and bathymetry data.

The links to download the raw data, bathymetry data, and all other derived data products have been documented in the section **Data Availability**.

RC2: Anonymous Referee #2:

General comments:

This paper sets out to define the sub-ice-shelf bathymetry beneath the Getz Ice Shelf using a combination of Operation ICE Bridge (OIB) and new helicopter-borne gravity data. It goes on to calculate ice-shelf basal melt rates and discuss the links to sub- glacial bathymetry and freshwater discharge from beneath the grounded ice sheet.

The overall concept of this paper is good, and the correlation of predicted onshore- melt pathways and ice shelf channels is striking. However, recovery of sub-ice-shelf bathymetry is challenging. A number of points regarding the inversion method should therefore be addressed and clarified before publication. In addition the assertion that "the pattern of basal melt is correlated with bathymetric troughs" and that ice-shelf basal melt is concentrated in "deep troughs" is not clearly backed up by the presented figures.

Thank you. We have expanded the section on the recovery of sub-ice shelf bathymetry according to the specific comments. The list of main changes is listed on page one of this report. In addition, we have rephrased the sentences on the relationship between the melt rate and the factors that affect the melt rate of Getz, including bathymetry, ice draft, and subglacial discharge (see below the responses to the specific comment on L147 -148).

Specific comments:

L61-62 "The gravity anomaly follows the topography in this region quite well (Fig. S2), which suggests the effectiveness of combining OIB and helicopter data".

Fig. S2 shows the gravity data overlain by the satellite imagery. It therefore does not strictly show that the gravity anomaly follows the topography. Rather it shows that the gravity highs are clearly associated with regions of ice shelf grounding and more elevated islands within the ice shelf system.

In addition this image (Fig. S2) does not really show the effectiveness of combining OIB and helicopter data. A shaded relief map of the free air gravity data with no satellite overlay would be significantly more revealing of the quality of the join between the OIB and helicopter data. I would strongly recommend adding this at least to the supplementary material. The subsequent cross-over analysis does confirm the two data sets match well, but this cannot be seen from the presented figure.

We agree that Fig. S2 doesn't strictly show gravity anomaly follows topography everywhere. So, we deleted the original sentence "The gravity anomaly follows the topography in this region quite well (Fig. S2)".

We've revised Fig. S2 to be a shaded relief map of free-air gravity data with no underlying satellite imagery. The shaded relief view shows the quality of combining the OIB and helicopter datasets is good over the trough area between Dean Island and Siple Island.

Section 2.2 Bathymetric Inversion Approach.

Given that 2D modelling underpins the inversion approach this section should be expanded. Firstly at least some of the constructed 2D models should be shown as supplementary figures. These should include input gravity, constraining radar derived topography or swath derived bathymetry if available, and the resulting modelled gravity field. This would give significant confidence in the robustness of the recovered bathymetry. In addition it is not clear if all, or only some of the flight lines shown in Figure 1 were modelled, or if the models were constructed separately using the gridded gravity data. Locations of actual models could simply be highlighted in Figure 1.

As the reviewer suggested, we added 2D models as supplementary figures (Fig. S4). We show gravity lines from both OIB and helicopter gravity surveys. In the upper panel, we present input gravity and resulting modeled gravity. In the lower panel, we show radar-derived ice topography and inverted bathymetry. See Fig. S4 of the supplementary information.

In addition, we highlighted the locations of actual gravity lines as black dashed lines in Figure 1.

It is not clear if/how the different bathymetric 2D profile models are tied together. Were the models forced to the same level at intersecting points, or were the different derived bathymetric profiles simply merged through a gridding process? This latter strategy could introduce gridding artefacts – see next point. Adding the offsets at profile intersections could be a good additional estimate of the robustness of the 2D modelling method.

Agreed. It was not clear enough how different bathymetric 2D profiles modes are tied together. The derived bathymetric profiles from each 2D model were merged through a gridding process by the minimum curvature gridding method. However,

gridding could introduce artifacts at the intersection points. We calculate the offset the profile intersection and the average offset is about 20 m. We added one paragraph on how the bathymetric grid was created - see next response.

How was the bathymetric grid presented created, i.e. what interpolation method was used (e.g. spline, kriging, nearest neighbour). What was the grid mesh size of the interpolated grid? Were any steps implemented to prevent aliasing and high frequency signals on the lines generating spurious patterns in the derived bathymetric grid?

As mentioned in the previous response, minimum curvature was used as the interpolation method to create the bathymetric grid. The grid mesh size of the interpolated grid is 1792 m. To de-alias, we did two things: increase the low-pass de-sampling factor and set the blanking distance to not include the over-shoot areas of the grid. We have added one paragraph on how the grid was created, stating that,

"The different 2D bathymetric profiles are merged through the minimum curvature gridding method, provided by the *Grid and Images* module from Geosoft Oasis montaj. The details of the minimum curvature method can be found in Briggs (1974). The mesh size of the interpolated grid is 1792 m. To prevent aliasing and high frequency signals, we increase the low-pass de-sampling factor (i.e., the number of grid cells that are averaged). This factor (set to 3) removes high frequency signals since it acts as a low-pass filter by averaging all point into the nearest cell. The distance between grid cells and a valid point greater than the blanking distance (set to 2000 m) are blanked out in the final grid. However, gridding could still introduce artifacts at the intersection points. We calculate the offsets at the profile intersections, and the average offset is about 20 m."

Related to the point above was onshore line radar data, or offshore swath bathymetric data included in generating the final bathymetric grid (beyond constraining the 2D gravity models)? This would be my recommendation, as it will help generate a seamless transition between the 'observed' bathymetry and the bathymetric estimates derived from gravity data.

Yes, IBCSO was included to help generate the final bathymetric grid. We have added the description of the final bathymetry grid, stating that "The final derived bathymetry (Figure 1a) includes the Getz Ice Shelf bathymetry from gravity inversion and offshore bathymetry from IBCSO (International Bathymetric Chart of the Southern Ocean) (Arndt et al., 2013)."

Was any pre-processing done on the gravity data to account for long wavelength geological factors such as sedimentary basins or changes in crustal thickness? Such factors might be expected in a region like the Getz Ice Shelf which is relatively close to the continent ocean boundary.

There was no pre-processing done on the gravity data to account for long wavelength geological factors such as a major sedimentary basin or crustal thickness gradient. Although our methods do account for local geological heterogeneity (see the response to the densities question below), our confidence that neither longer wavelength effects or shorter wavelength draping of marine sediments are significant are described in the following added paragraph.

"We do not include significant geological or sedimentary signatures in our model since we have insufficient magnetic analysis over Getz. But our methods do account for local geological heterogeneity (see Supplementary Fig. S3). Published interpretations within ASE (Amundsen Sea Embayment) imply that we should not expect a significant crustal thickness gradient or sedimentary basin lies beneath the Getz Ice Shelf (Gohl et al., 2013). Therefore, we expect sediments near the grounding line being scoured away as seen in other ice shelves of ASE (Gohl et al., 2013; Cochran et al., 2014). However, if the sediment is present, it will cause the gravity-derived bathymetry to be deeper than the actual seafloor. Our uncertainty estimates (see Supplementary Fig. S4) indicate that our gravity derived bathymetry is shallower than both the measured off-shore bathymetry and the measured bed elevation beneath the grounded ice adjacent to Getz. If we are correct and no significant geological structure underlies the Getz then the existence of sediments will shift the bathymetry to be deeper but will not change the shape of the bathymetry, and thus will not affect our conclusions."

Figure 2c. In addition to the basal melt rate and bathymetry it would be good to show the free air gravity field along this profile. This would give additional confidence in the inversion result, as individual bathymetric features could be linked to observed gravity anomalies.

We added free air gravity field along profile XYZ to Figure 2c. Free air gravity anomaly is relatively low along both XY and YZ, which are over the deep troughs. The free air gravity anomaly is higher over the sill area. We added this link to the corresponding result section, which states, "The free-air gravity field also reflects the general shape of the bathymetric features (Fig. 2c). Along the profile XYZ

(Fig. 2c), the bathymetric sill has higher gravity anomaly values. The trough area has low gravity anomaly values."

L75-76 "The bathymetry model is updated iteratively until the difference between modeled gravity and observed gravity values is minimized". What is the limit on this convergence? Typically this should be (at most) the error of the observed data. Allowing the model to fit the data more precisely runs the risk of over-fitting the anomalies with more extreme topographic undulations not truly supported by the data.

We have added the convergence limit to the original sentence, which states, "The bathymetry model is updated iteratively until the difference between modeled gravity and observed gravity values is minimized (convergence limit = 0.1 mGal, 0.1 mGal is the standard error of observed gravity data)."

L79 and Fig. S3 denotes the polygon densities applied in this region. How were these densities chosen? The densities presented are significantly higher than the standard Bouguer correction (2670 kgm-3) which is generally accepted as the typical density of upper continental crust. Use of an unreasonably high rock density could lead to underestimation of the true amplitude of the bathymetry. The presence of apparent volcanic cones on the islands would suggest a higher than usual density (depending on lithology), however, granites seen in outcrop just the west of the survey region would indicate a density closer to the continental crustal average would be suitable. Some discussion of where these numbers come from is therefore needed.

One of the challenges of inverting gravity data for bathymetry models is that the densities of any geology below the water bottom are unknown. We follow the strategy of Greenbaum (2015) by first obtaining density models of bedrock from survey lines over grounded-ice areas. We then use these densities to invert for bathymetry models for survey lines over the floating-ice areas adjacent to the grounded ice density determinations. The assumption of this approach is that no significant difference in bedrock densities exist in adjacent grounded-ice and floating-ice areas. Therefore, we have added new paragraphs on where the polygon density values come from, which states,

"We first use the gravity data from grounded ice lines to invert for bedrock densities. For those areas covered by the grounded ice lines, we assume a three-layer model: a solid ice layer with density of 0.917 g/cm$_3$ of known thickness over a bedrock layer, whose density is our free parameter; the third layer is the upper

mantle with a density of 3.3 g/cm$_3$ at a depth of 20 km. The top, bottom, and thickness of the ice layer is obtained from OIB measurement and thus fixed throughout the inversion. We start the inversion with an initial guess of granitic rock density value 2.75 g/cm$_3$ since west of the survey area has granite outcrop (Mukasa et al., 2000).

The gravity data from floating ice lines is used to invert for the bathymetry under Getz. We use a four-layer model: the first layer is an ice layer with density of 0.917 g/cm$_3$ with a known depth; the second layer is a seawater layer with a density of 1.03 g/cm$_3$, the depth of this layer is our free parameter; the third layer is a bedrock layer with density inferred from grounded-ice-line gravity data; the fourth layer is the upper mantle with a density of 3.3 g/cm$_3$ at a depth of 20 km. The lines are processed one by one starting from those that are closer to grounded ice lines."

L129 Talking about the least squares relationship between ice shelf thickness and melt rate. What is the quality of this fit (e.g. r2 value)? It would be good to show the trend line over the data point cloud to allow a more intuitive assessment of this fit.

Reviewer 1 also identified that this paragraph needed attention (above: Line 127-132). As we describe in the response above, we have addressed the issue by removing this problem paragraph from the text.

L147-148 states "We discover that melt is concentrated along the grounding line of Getz and in deep troughs". Also L185-186. Figure 2b does show melt concentrated near the grounding line. However, it is not totally clear that melt is associated with all the deep troughs identified in the gravity data. For example in Fig. 2b along profile X-Y melt rate is relatively low, but this region is underlain by a major trough. In contrast Fig. 2c shows that the peak in melt rate around Y is associated with relatively shallow bathymetry. In addition the very deep trough identified east of Wright Island is not associated with very major basal melting, despite the ice shelf being >500m deep. It is probably fine to say deep troughs are present allowing warm water to access the grounding line region, but this is not a clear correlation between melting and deep troughs.

Agreed. Only some of the troughs in the Getz area correspond to a high melt rate, but high melt rate is often observed where these troughs intersect the grounding line. We have changed the original sentence from L147-148 from "We discover that melt is concentrated along the grounding line of Getz and in deep troughs." to

“We discover that melt is concentrated along the grounding line, especially where it intersects deep troughs.”

To have a clearer discussion of the relationship between melt rate and the factors that impact the melt rate, we have also rephrased the original L185-186 of section 4.2. Also, we have added an explanation of why Fig. 2c shows a melt rate around Y, which is associated with shallow bathymetry. These updates are reflected in the following paragraphs, which states,

“Previous oceanographic surveys have shown that the Getz melt rate is sensitive to ocean temperature, thermocline depth, circulation strength, bathymetry, and ice thickness (Jacobs et al., 2013). In our study, the factors that may affect the melt rate over the trough area are bathymetry, ice bottom elevation, incursion of warm water, subglacial discharge drained across the grounding line, and the continuity of the troughs from the grounding line to the ice shelf edge (Fig. 2 and Fig. 3). Differences in melt regimes are apparent between the two troughs we report. Most notably, ice in the DWT experiences a much higher melt rate than ice in the SDT, likely because the deep draft of the Eastern Getz places it in warm CDW, whereas the shallow base of the ice to the west sits in relatively cooler water. In Eastern Getz, the high basal melt region over DWT corresponds to thick ice, where the base sits in the water below the 500 m thermocline depth (stippled region in Fig. 2b).

The existence of a trough does not necessarily indicate that the melt rate will be high over it. XY is overlain by a deep trough and allows the incursion of CDW with high melt rate at the grounding line. However, the ice draft is shallower than the thermocline depth, so we do not observe high melt rate all along the trough overlain by XY. Similarly, the melt rate is high over DWT since the ice draft is deeper than the thermocline depth. In addition, subglacial hydrological modeling (Figure 3) suggests that the subglacial meltwater from upstream may drain through channel B and enhance the melt rate near Y. Therefore, although Y has a relatively shallow bathymetry, we observe a melt rate peak around Y.

Besides, we have added new explanation of why the deep trough which lies east of Wright Island does not appear a high melt rate to section 4.1 (Continuity of the troughs) and 4.2. The new sentences added to section 4.1 states,

“One exception is the deep trough that is identified east of Wright Island, where the depth of trough is ~200 m shallower than the trough of the inner continental shelf near the ice shelf front.”

The new sentences added to section 4.2 states,

“In addition, the deep trough that is identified east of Wright Island does not correspond to a high melt rate. There is no pathway for CDW intrusion to the ice shelf cavity over that deep trough since the trough is not continuous from the inner continental shelf to the ice shelf cavity. Therefore, the deep trough that lies east of Wright Island is not associated with a major basal melting although the corresponding ice draft is deep (Fig. 2b).”

Technical corrections:

L31 “feasibility of gravity observations from a ship at sea” would be better as “feasibility of gravity observations from a helicopter operating from a ship at sea”

Changed as suggested.

L36 “By pairing location. . .. . ..” might be better as “By comparing locations. . ...”

Changed as suggested.

L42-43 This sentence appears to repeat itself.

The repeated sentence is deleted.

L51 “non-discharge melt rates”. This is the 1st introduction of this term, which I did not find self-explanatory. I would suggest either defining it here, or simply saying: “The observed basal melt rates were computed using a mass conservation approach from Jenkins (1991) and Gourmelen et al. (2017b), and corrected for melting driven by warm ocean waters using ice bottom elevation and nearby ocean temperature profiles (Holland et al., 2008)”.

We adopted the reviewer’s latter suggestion. Here we simply say “The observed basal melt rates were computed using a mass conservation approach from Jenkins (1991) and Gourmelen et al. (2017b), and corrected for melting driven by warm ocean waters using ice bottom elevation and nearby ocean temperature profiles (Holland et al., 2008).” The term “discharge melt rate” is defined up-front in its corresponding section – see below the response to comment on L107/108.

L97 "The observed basal melt rates" might be better as "the observed ice-shelf basal melt rates" to distinguish this calculation from anything onshore.

Changed to "the observed ice shelf basal melt rate".

L107/108 I would define "non-discharge melt rate" up-front at this point, as it is some- what confusing, until it is explained.

Agreed. "Non-discharge melt rate" is defined here up-front: "We modeled the melt rates over Getz that are expected to result from the in situ farfield ocean temperature. We refer to this modeled melt rate as non-discharge melt rate through this paper since it does not consider any potential impact from local subglacial discharge."

L154 Suggest subheading should be "Melt rate with no sub-glacial discharge".

We have changed the subheading to "Melt rate with no sub-glacial discharge".

L215 "Therefore, a similar study over other massive ice shelves such as Getz should be addressed in the future" might be better as "Therefore, a similar study over other massive ice shelves similar to Getz should be addressed in the future".

Changed as suggested.

All maps – it would be useful to have the coastlines of the islands shown, not just the edge of the ice shelf.

We have updated almost all maps with the coastlines of the islands except Fig. 2b, in which islands are identifiable from the background satellite image and are labeled with their names.

Getz Ice Shelf melt enhanced by freshwater discharge from beneath the West Antarctic Ice Sheet

Wei Wei[1], Donald D. Blankenship[1], Jamin S. Greenbaum[1], Noel Gourmelen[2], Christine F. Dow[3], Thomas G. Richter[1], Chad A. Greene[4], Duncan A. Young[1], SangHoon Lee[5], Tae-Wan Kim[5], Won Sang Lee[5], and Karen M. Assmann[6]

[1]Institute for Geophysics and Department of Geological Sciences, Jackson School of Geosciences, University of Texas at Austin, Austin, TX, United States.
[2]School of Geosciences, University of Edinburgh, Edinburgh, United Kingdom.
[3]Department of Geography and Environmental Management, University of Waterloo, Waterloo, Ontario, Canada.
[4]Jet Propulsion Laboratory, California Institute of Technology, Pasadena, California, United States.
[5]Korea Polar Research Institute, Incheon, South Korea.
[6]Department of Earth Sciences, University of Gothenburg, Gothenburg, Sweden.

Correspondence: Wei Wei (wwei@utexas.edu)

Abstract. Antarctica's Getz Ice Shelf has been rapidly thinning in recent years, producing more meltwater than any other ice shelf in the world. The influx of freshwater is known to substantially influence ocean circulation and biological productivity, but relatively little is known about the factors controlling basal melt rate or how it is spatially distributed beneath the ice shelf. Also unknown is the relative importance of subglacial discharge from the grounded ice sheet in contributing to the export of freshwater from the ice shelf cavity. Here we compare the observed spatial distribution of basal melt rate to a new sub-ice shelf bathymetry map inferred from airborne gravity surveys and to locations of subglacial discharge from the grounded ice sheet. We find that melt rates are high where bathymetric troughs provide a pathway for warm Circumpolar Deep Water to enter the ice shelf cavity, and that melting is enhanced where subglacial discharge freshwater flows across the grounding line. This is the first study to address the relative importance of meltwater production of the Getz Ice Shelf from both ocean and subglacial sources.

1 Introduction

The Getz Ice Shelf (Getz, herein) in West Antarctica is over 500 km long and 30 to 100 km wide; it produces more freshwater than any other source in Antarctica (Rignot et al., 2013; Jacobs et al., 2013; Assmann et al., 2019), and in recent years its melt rate has been accelerating (Paolo et al., 2015). The fresh, buoyant water that emanates from the Getz cavity drives regional and global ocean circulation (Nakayama et al., 2014; Jourdain et al., 2017; Silvano et al., 2018) while providing critical nutrients for biological production (Raiswell et al., 2006), but little is known about the origins or sensitivities of this major freshwater

source. Specifically, the variability of freshwater from ice shelf melt has not been modeled due to poorly constrained bathymetry beneath the ice shelf, which has resulted in a poor understanding of how water circulates throughout the ice shelf cavity. And to date, despite the major role that freshwater from Getz plays in the Southern Ocean, no studies have considered the contribution of subglacial meltwater that originates beneath grounded ice, nor its role in influencing the circulation and melt patterns beneath the ice shelf.

To understand the potential pathways for warm ocean water to enter in the Getz cavity we conducted a bathymetric survey using a ship-based, gravimeter-equipped helicopter. As part of a collaboration between the University of Texas Institute for Geophysics (UTIG) and Korea Polar Research Institute (KOPRI), an AS350 helicopter was outfitted with an aerogephysical instrument suite adapted from a design which has previously been operated from fixed-wing aircraft (Greenbaum et al., 2015; Tinto and Bell, 2011). Operating from the RVIB Araon off the Getz coast (see Supplementary Fig. S1), the survey covered areas between Dean Island and Siple Island located in the west of Getz (green lines in Fig. 1) and crossed existing coast parallel Operation IceBridge (OIB) lines (blue lines in Fig. 1). Gravimetry from helicopter platform can achieve higher resolution of 3 km than conventional fixed wing surveys with resolution of 4.9 km due to lower flying speed of helicopter. This is the first ever demonstration of the technical and logistical feasibility of gravity observations from a helicopter operating from a ship at sea to obtain high resolution gravity data over an Antarctic ice shelf.

We used the airborne gravity data to infer the bathymetry beneath Getz (see methods on the bathymetry inversion approach). We also developed a new high-resolution map of Getz basal melt rates using satellite radar altimetry data from the years 2010 to 2016 (see methods on the observed basal melt rate) to understand where ice shelf melt may be correlated with underlying bathymetry. By ~~pairing~~ comparing locations and rates of melt with our new understanding of the Getz cavity bathymetry, we gain first insights into where ice shelf melt is dominated by contact with Circumpolar Deep Water (CDW) and where bathymetry blocks the flow of CDW. We also considered the potential role of subglacial discharge as a mechanism that can cause locally enhanced melt rates (Le Brocq et al., 2013; Marsh et al., 2016). We used the Glacier Drainage System (GlaDS) model, which simulates co-evolution of subglacial distributed and channelized drainage networks that have been demonstrated to correspond well with geophysical data of basal water systems (Dow et al., submitted). We applied this model to estimate the production rate and spatial distribution of subglacial meltwater (Werder et al., 2013; Dow et al., 2016, 2018) ~~, to model the production rate and spatial distribution of subglacial meltwater~~ (see methods on the subglacial hydrological model). We then compared the spatial distribution of observed ice shelf melt to locations and flux rates from subglacial discharge locations predicted by GlaDS.

2 Methods

We present three types of data in the study: the spatial distribution of basal melt rate (see Fig. 2b and Fig. 3) , bathymetry inferred from airborne gravity surveys (shown in Fig. 2a), and locations of subglacial discharge (see Fig. 3) from the grounded ice sheet. We inferred the bathymetry of Getz using profile gravity inversions with the Geosoft GMSYS software. The subglacial hydrological analysis was generated by the two-dimensional GlaDS (Glacier Drainage System model) (Werder et al.,

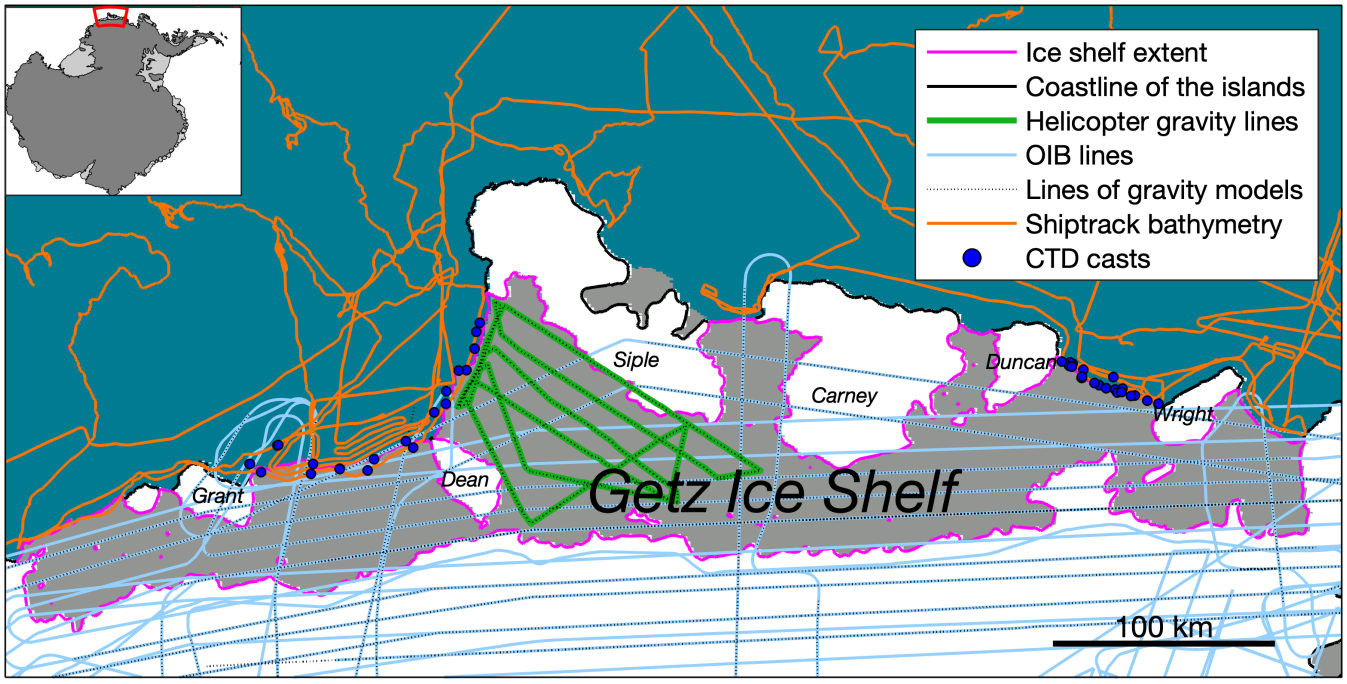

Figure 1. The geographic location and data coverage of Getz. The blue area is ocean. The gray area is Getz Ice Shelf. The white area is grounded ice. Coloured lines and marks denote the ice shelf extent (Mouginot et al., 2017), helicopter gravity data, and NASA OIB data (Cochran and Bell, 2010), shiptrack bathymetry (Nitsche et al., 2007) and CTD casts (Locarnini et al., 2013). This plot is generated from Antarctic Mapping Tool (Greene et al., 2017).

2013). The observed basal melt rates were computed using a mass conservation approach from Jenkins (1991) and Gourmelen et al. (2017b). The non-discharge melt rates were estimated from , and corrected for melting driven by warm ocean waters using ice bottom elevation and nearby ocean temperature profile profiles (Holland et al., 2008).

2.1 Helicopter gravity data acquisition

The gravity data used in this paper was acquired aboard two aircraft types, one fixed-wing aircraft and one helicopter. Fig. 1 shows the data coverage. The OIB data (Cochran and Bell, 2010) was acquired using the Sander Geophysics Limited (SGL) AIRGrav system aboard NASA's DC-8. More details of this airborne geophysical platform can be found in the literature (Cochran and Bell, 2012; Cochran et al., 2014). The helicopter based data was acquired using a Canadian Micro Gravity GT-1A in a collaboration between the University of Texas Institute for Geophysics (UTIG) and Korea Polar Research Institute (KOPRI). Fig. S1 shows the helicopter gravity data acquisition platform on the icebreaker Araon. Three dedicated aerogeophysical flights were accomplished in one day of helicopter operations from the Araon while off the coast of the Western Getz, acquiring about 1200 line-kilometers of data. The gravity anomaly follows the topography in this region quite well (Fig. S2) , which suggests the effectiveness of combining OIB and helicopter data. The observed gravity anomaly ranges from -60 mGal

to 30 mGal (Fig. S2). The high anomaly strongly correlates with the ice rises and grounded icebergs. Large positive gravity anomalies of up to 30 mGal are consistently found over Grant Island, Dean Island, Siple Island, and Wright Island. The areas between ice rises correspond to low gravity anomalies.

Both survey data sets show similar repeatability statistics with ∼1.4 to 1.6 mGal root mean square (RMS) in the differences at crossovers between lines both internally in each set and between sets. The ship based UTIG/KOPRI gravity set did not have an absolute gravity tie so that entire survey set was level shifted to minimize the difference in the mean of crossovers with the OIB data; no other adjustments were done.

2.2 Bathymetry inversion approach

The gravity data is inverted for depth of targets using the GM-SYS Profile Modeling, a 2D gravity modeling and inversion module in Geosoft. In the forward modeling mode, the module computes the gravity response from a polygon approximated irregular target model (Talwani et al., 1959). In the inversion mode, the polygon approximated model is adjusted iteratively to best fit the observed gravity data. Getz is pinned on an array of islands and peninsulas, so our bathymetry inversion is well constrained by the location of the ice rises and the peninsulas. The bathymetry model is updated iteratively until the difference between modeled gravity and observed gravity values is minimized (convergence limit = 0.1 mGal, 0.1 mGal is the standard error of observed gravity data). To better condition the inversion process, we fix the top and bottom of the ice layers, whose depth and topography are obtained from radar data. Similar approaches to infer bathymetry from airborne gravity data have been applied in many regions of Antarctica (Tinto and Bell, 2011; Cochran and Bell, 2012; Muto et al., 2016; Millan et al., 2017; Greenbaum et al., 2015). ~~The~~

We first use the gravity data from grounded ice lines to invert for bedrock densities. For those areas covered by the grounded ice lines, we assume a three-layer model: a solid ice layer with density of 917 $kg \cdot m^{-3}$ of known thickness over a bedrock layer, whose density is our free parameter; the third layer is the upper mantle with a density of 3300 kg·m at a depth of 20 km. The top, bottom, and thickness of the ice layer is obtained from OIB measurement and thus fixed throughout the inversion. We start the inversion with an initial guess of granitic rock density value 2.75 kg·m since west of the survey area has granite outcrop (Mukasa and Dalziel, 2000).

The gravity data from floating ice lines is used to invert for the bathymetry under Getz. We use a four-layer model: the first layer is an ice layer with density of 0.917 kg·m with a known depth; the second layer is a seawater layer with a density of 1030 kg·m, the depth of this layer is our free parameter; the third layer is a bedrock layer with density inferred from grounded-ice-line gravity data; the fourth layer is the upper mantle with a density of 3300 kg·m at a depth of 20 km. The lines are processed one by one starting from those that are closer to grounded ice lines. The bathymetry model is updated iteratively until the difference between modeled gravity and observed gravity values is minimized (convergence limit = 0.1 mGal, 0.1mGal is the standard error of observed gravity data). The polygon densities applied in this region is in Fig. S3. The constructed 2D models can be found in Fig. S4.

The different 2D bathymetric profiles are merged through the minimum curvature gridding method, provided by the Grid and Images module from Geosoft Oasis montaj. The details of the minimum curvature method can be found in Briggs (1974)

. The mesh size of the interpolated grid is 1792 m. To prevent aliasing and high frequency signals, we increase the low-pass de-sampling factor (i.e., the number of grid cells that are averaged). This factor (set to 3) removes high frequency signals since it acts as a low-pass filter by averaging all point into the nearest cell. The distance between grid cells and a valid point greater than the blanking distance (set to 2000 m) are blanked out in the final grid. However, gridding could still introduce artifacts at the intersection points. We calculate the offsets at the profile intersections, and the average offset is about 20 m. The final derived bathymetry (Fig. 2a) includes the Getz Ice Shelf bathymetry from gravity inversion and offshore bathymetry from IBCSO (International Bathymetric Chart of the Southern Ocean) (Arndt et al., 2013).

We follow the uncertainty estimation approach from Greenbaum et al. (2015). We compare the inversion with the geometry of the grounded ice as a measure of the uncertainty beneath the floating ice assuming that the bed roughness under grounded ice and floating ice are similar. Our estimated Root Mean Square Error (RMSE) between the ice bottom measured by radar and sampled from the bathymetry model is about 246 m and the mean offset between the two is about 44 m (see Supplementary Fig. ~~S4~~S5). We also compare the overlapping points where the gravity lines intersect with the shiptrack (Nitsche et al., 2007). The Root Mean Square Error (RMSE) between the ship measured bathymetry and sampled from the bathymetry model is about 121 m, the mean offset between the two is about 32 m (see Supplementary Fig. ~~S4~~S5).

We do not include significant geological or sedimentary signatures in our model since we have insufficient magnetic analysis over Getz. But our methods do account for local geological heterogeneity (see Supplementary Fig. S3). Published interpretations within ASE (Amundsen Sea Embayment) imply that we should not expect a significant crustal thickness gradient or sedimentary basin lies beneath the Getz Ice Shelf (Gohl et al., 2013). Therefore, we expect sediments near the grounding line being scoured away as seen in other ice shelves of ASE (Gohl et al., 2013; Cochran et al., 2014). However, if the sediment is present, it will cause the gravity-derived bathymetry to be deeper than the actual seafloor. If we are correct and no significant geological structure underlies the Getz then the existence of sediments will shift the bathymetry to be deeper but will not change the shape of the bathymetry, and thus will not affect our conclusions.

2.3 Subglacial hydrological model

The subglacial hydrological analysis is generated by the two-dimensional GlaDS (Glacier Drainage System model) (Werder et al., 2013). Distributed flow occurs through linked cavities that are represented as a continuous water sheet of variable thickness. Channels grow along finite element edges and exchange water with the adjacent distributed system, as part of a fully coupled 2D drainage network. The model is run to the steady state over 3000 days with primary outputs being channel discharge over the domain and the grounding line into the Getz cavity. Topography inputs are from airborne radar data; basal velocity is estimated as 90% of MEaSUREs surface velocity data (Rignot et al., 2017); basal conductivity is assumed constant following other applications of GlaDS in Antarctica (Dow et al., 2016, 2018). Water input rate is set as constant (both spatially and temporally) at 10 $\mathrm{mm \cdot yr^{-1}}$ following geothermal flux rate calculations (Pattyn, 2010).

2.4 Observed basal melt rate

The observed ice-shelf basal melt rates are computed using a mass conservation approach from surface elevation, surface mass balance, ice velocity and ice shelf thickness (Jenkins, 1991; Gourmelen et al., 2017b), using the relation (Jenkins, 1991; Gourmelen et al., 2017b)

$$-\left(1-\frac{\rho_{\text{ice}}}{\rho_{\text{ocean}}}\right)\dot{m}+\text{SMB}=\frac{\partial S}{\partial t}+S\nabla\cdot\mathbf{u}, \tag{1}$$

where ρ_{ice} is ice density of 917 kg·m^{-3}, ρ_{ocean} is the ocean density of 1028 kg·m^{-3}, $\dot{m}$ is basal melt rate, SMB is surface mass balance, S is surface elevation and $\mathbf{u}$ is ice velocity. SMB is obtained from output of the regional atmospheric climate model RACMO2 (Van Wessem et al., 2016). We derive the rates of surface elevation change from a new elevation dataset, which is generated by the CryoSat-2 interferometric-swath radar altimetry from 2010 to 2016. Ice velocity is acquired from radar observation of the European Space Agency Sentinel-1a mission. A detailed discussion of the methodology can be found in Gourmelen et al. (2017a). The observed melt rate of Getz is shown in Fig. 2b.

2.5 Non-discharge melt rate

We modeled the melt rates over Getz that are expected to result from the in situ farfield ocean temperature. We refer to this modeled melt rate as non-discharge melt rate through this paper since it does not consider any potential impact from local subglacial discharge. Melt rate shown in Fig. 2b are dominated by ocean forcing. To the first order, melt rates are visibly related to ice basal depth, and accordingly we note that melt rates are high where the draft of the ice shelf dips below the ~500 m depth of the thermocline. As our interest is in exploring the possible mechanisms of melt beyond the first-order effects of ocean forcing, Fig. 3 shows melt rate ~~anomalies~~ residuals after the first-order influence of ocean temperature on melt has been removed.

Removing the first-order effects of ocean forcing from the basal melt rate distribution requires a model of the relationship between ocean temperature and observed melt rates. Several such models have been proposed, and have generally assumed a linear to quadratic relationship between ocean temperature and ice shelf melt rates (Holland et al., 2008). However, estimates determined empirically or through numerical models vary widely, likely due to influences such as basal slope (Little et al., 2009) and basal roughness (Gwyther et al., 2015), which may not be the same for all ice shelves. Here, we use data from Getz to develop only the simplest possible relationship between ocean temperature and melt rates, then we investigate where and how melt observations deviate from the simple first-order model.

To relate the observed melt rates to ocean forcing, we obtain temperature profiles from 25 CTD casts taken within 6 km of Getz. We converted in situ temperatures to pressure- and salinity-dependent temperatures above freezing using the Gibbs-SeaWater Oceanographic Toolbox (McDougall and Barker, 2011). The 25 profiles of $\mathsf{T}-\mathsf{T}_{\text{freeze}}$ are shown in Fig. 2c. The mean profile of $\mathsf{T}-\mathsf{T}_{\text{freeze}}$ was then used to interpolate the local temperature above freezing corresponding to the depths of the basal ice in each grid cell of Getz. Ice basal depths were calculated assuming hydrostatic equilibrium for ice of 917 kg·m^{-3} density in seawater of 1028 kg·m^{-3} density, using REMA surface elevations (Howat et al., 2019) that we converted to the GL04C

geoid (Förste et al., 2008; Greene et al., 2017) and from which we removed modeled firn air content (Ligtenberg et al., 2011). The resulting estimated basal temperature distribution is shown in Fig. ~~S5~~S6.

~~From the basal temperature distribution shown in Fig. S5 and the observed melt rate distribution shown in Fig. 2b, we computed a simple linear least-squares relationship constrained to (0,0) using the `polyfitw` function in the Climate Data Toolbox for MATLAB (Greene et al., 2019). The least-squares fit yielded a relationship of 3.8 m$\cdot$yr$^{-1}\cdot$K^{-1}. This value is lower than many estimates that have previously been determined through models or targeted measurements (Holland et al., 2008). We note that the relationship we find represents an area-averaged value for the entire ice shelf, so it is not surprising to find a lower value than studies that have focused on steep basal slopes close to the grounding line.~~

3 Results

3.1 The new Getz bathymetry

The new map of airborne gravity-derived bathymetry is shown in Fig. 2a. The inversion reveals deep troughs are continuous from the inner continental shelf to beneath the ice shelf. In Western Getz we identify a 1300 m deep trough between Siple Island and Dean Island, which we refer to as Siple-Dean Trough (SDT). In Eastern Getz we find a 1200 m deep trough between Duncan Peninsula and Wright Island, which we refer to as Duncan-Wright Trough (DWT). Published shiptrack bathymetry (Nitsche et al., 2007) shows that the Dotson-Getz Trough on the inner continental shelf extends to the ice front, and our results suggest that DWT is the continuation of the Dotson-Getz Trough, providing a pathway for CDW to enter to the ice shelf cavity without obstruction. Similarly, SDT is the continuation of the the West Getz Trough in which unmodified CDW has been reported (Assmann et al., 2019). We note, however, that despite the similar depths and close proximity of DWT to SDT, the two troughs are not connected, but are separated by a bathymetric sill that rises to a depth of approximately 500 $\pm$ 240 m between Siple and Carney islands (Fig. 2a) (see methods for uncertainty estimation of the gravity inversion). The free-air gravity field also reflects the general shape of the bathymetric features. Along the profile XYZ (Fig. 2c), the bathymetric sill has higher gravity anomaly values. The trough area have low gravity anomaly values.

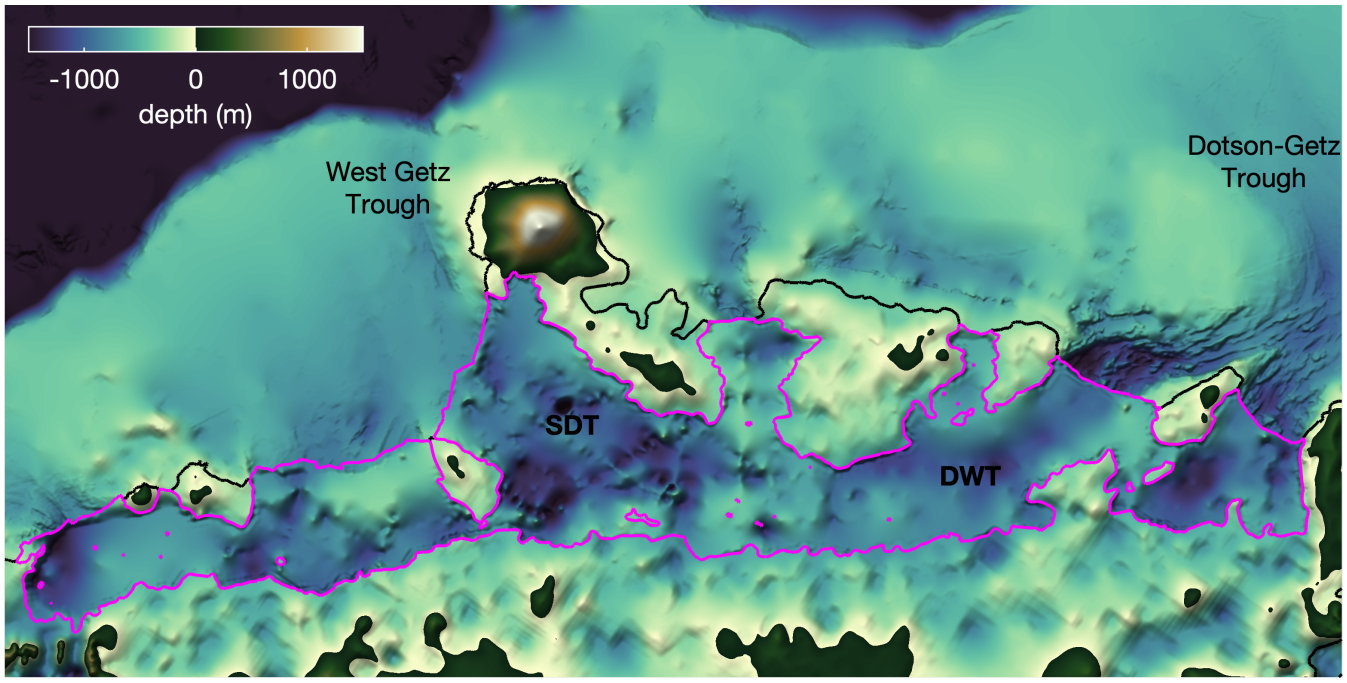
-1000
0
1000
depth (m)
West Getz
Trough
Dotson-Getz
Trough
SDT
DWT

(a)

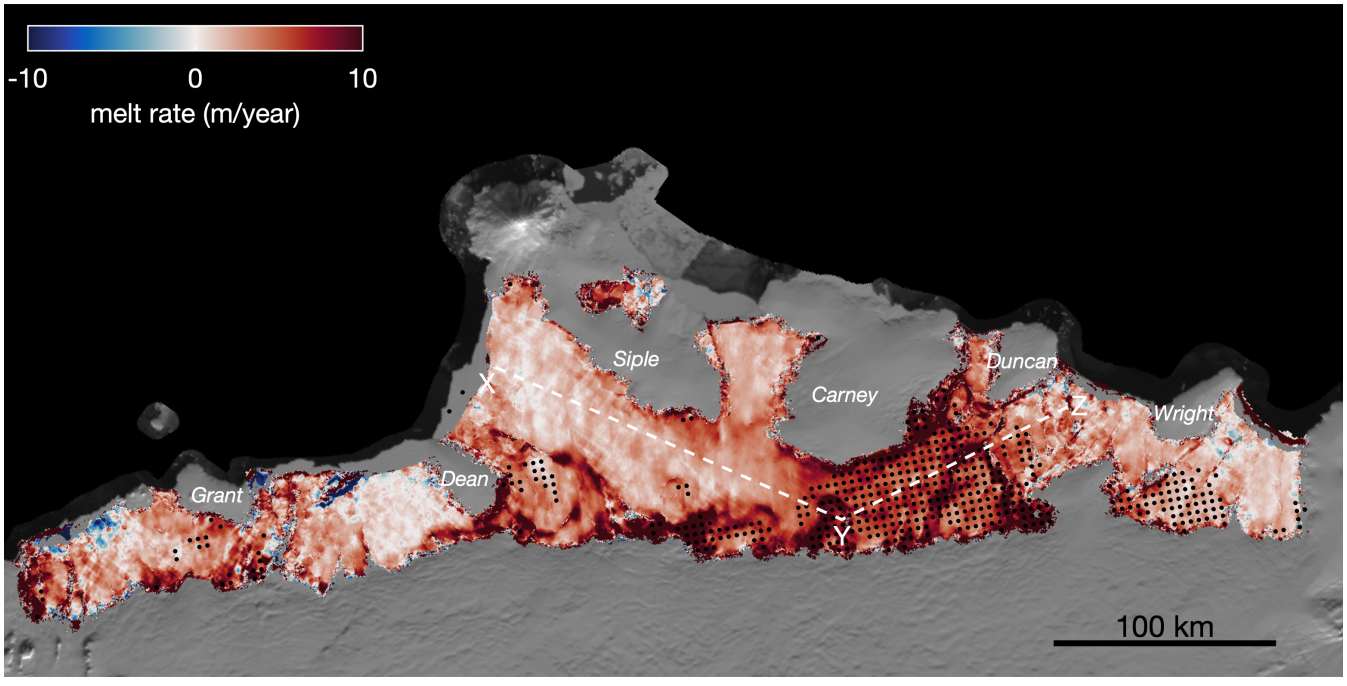
-10
0
10
melt rate (m/year)
Siple
Carney
Duncan
Wright
Dean
Grant
X
Y
Z
100 km

(b)

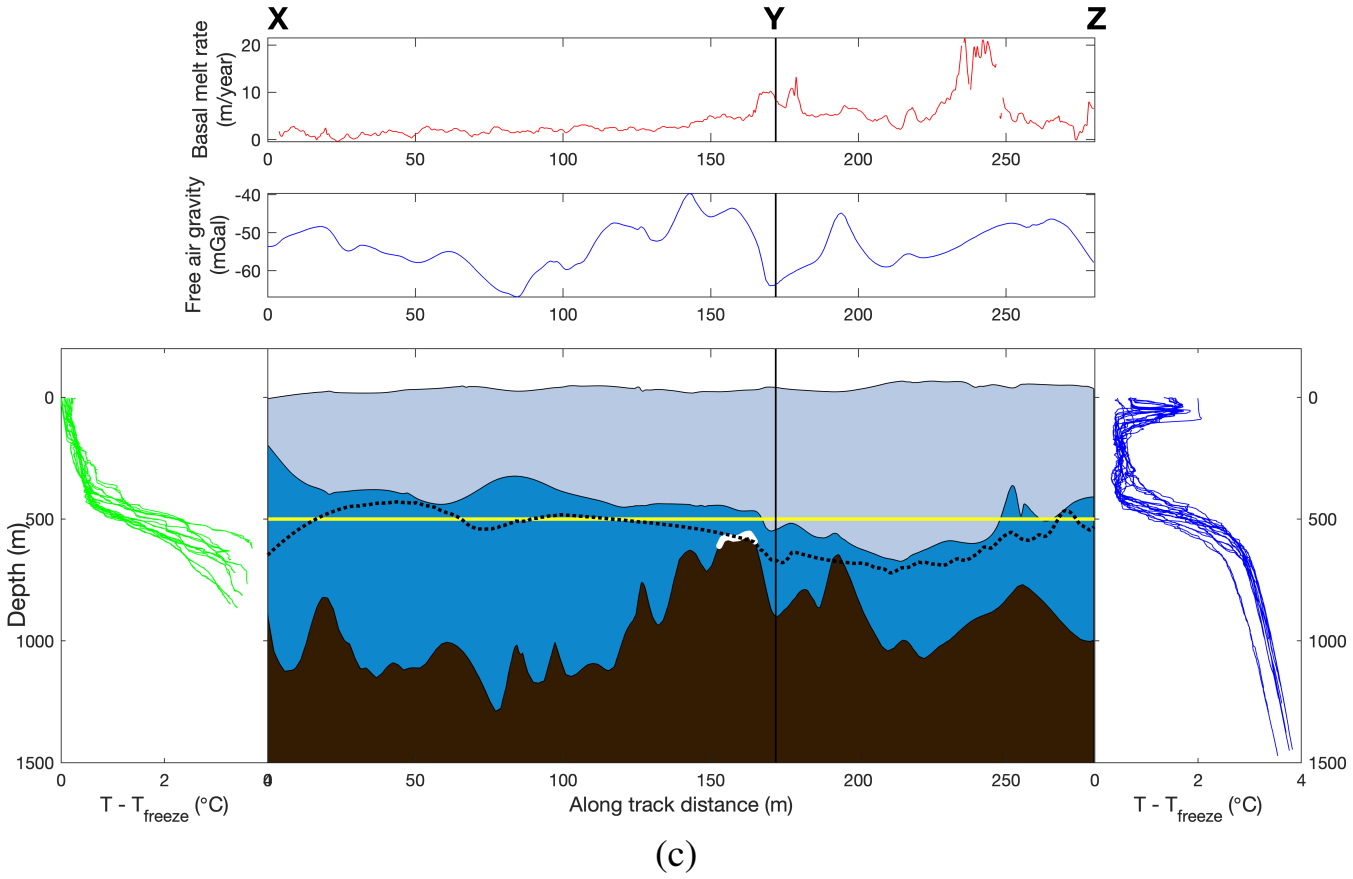

Figure 2. The shape of sea floor, basal melt rates and along profile view of the study area. (a) The bathymetry of the Getz Ice Shelf. The profile XYZ crosses the trough between Dean Island and Siple Island, the bathymetric sill, and the the trough between Duncan and Wright Islands. The purple is the ice shelf outline (Mouginot et al., 2017). The bathymetry of the continental shelf is from ~~RTOPO2~~ IBCSO (Arndt et al., 2013). (b) The observed basal melt rate. ~~The black stippled indicate the 500 m~~ Black stippling indicates ice bottom ~~elevation~~elevations deeper than 500 m. The background is the MODIS-derived Mosaic of Antarctica (MOA) (Scambos et al., 2007). (c) Upper panel shows the basal melt rate along profile XYZ. The lower panel shows the elevations of ice and bedrock along profile XYZ, with the depth temperature profiles from Western and Eastern Getz. Ocean is blue, ice is light blue, and the bedrock is brown. The white indicates the location of the bathymetric sill. The black dash line is the bathymetry from Bedmap2 (Fretwell et al., 2013). The horizontal yellow line indicates the mean thermocline depth.The thermal forcing $T - T_{freeze}$ is calculated from CTD casts (Locarnini et al., 2013).

3.2 The melt rates of Getz

3.2.1 Melt rate from observation

Fig. 2b shows our observation of mean basal melt rates from 2010 to 2016. We discover that melt is concentrated along the grounding line ~~of Getz and in~~ especially where it intersects deep troughs. The area-averaged melt under Getz is 4.15 $m \cdot yr^{-1}$,

equating to 141.17 Gt·yr^{-1} of freshwater flux into the Southern Ocean. We find a continuous channelized melt pattern (shown as the dark red in Fig. 2b), from the grounding zone to Eastern Getz calving front. The profile XYZ shown in Fig. 2c is sampled along SDT, the sill, and DWT. The top of the sill sits slightly below the 500 m thermocline depth, and may therefore allow exchange of warm deep waters between the Eastern and Western Getz. Fig. 2b shows that the 500 m ice bottom elevation, represented by the stippled, marks a boundary between low and high melt rates, likely resulting from the warm waters that reside below that depth.

3.2.2 Melt rate with no sub-glacial discharge

To understand how subglacial discharge might affect the melt rate of Getz, we compared the spatial distribution of basal melt observations to the patterns of melt that are expected to result from a simple depth-dependent model of melt rates (Holland et al., 2008). The simple model assigns melt rates based on the ice shelf draft and a corresponding depth-dependent water temperature (see Supplementary Fig. ~~S5~~S6), taken as the mean profile of several nearby oceanographic temperature measurements (Locarnini et al., 2013) (see methods on the non-discharge melt rate). We refer to this modeled melt distribution as the "non-discharge case" because it assumes melt is driven only by the in situ farfield ocean temperature, and does not consider any potential role of local subglacial discharge. Fig. 3 shows the difference between the non-discharge case melt rate and the observed melt rate. The areas where the observed melt rate exceeds the non-discharge melt rate (red area in Fig. 3) correspond to locations of subglacial discharge predicted by GlaDS.

3.3 The subglacial discharge locations v.s. the melt rate difference

GlaDS predicts subglacial discharge from several major subglacial channels that line up closely with the high melt regions at the ice shelf grounding line. Channel A near Grant Island has the largest channelized relative discharge rate of about 5.3 m^3·s^{-1}, while the channel outlets near the grounding line between Carney Island and Duncan Peninsula has relative discharge rates ranging from 1.76 to 2.4 m^3·s^{-1}. Channel B near the east of the bathymetric sill has a relative discharge rate of 1.76 m^3·s^{-1}. These channel outlets and relative discharges match up with ice shelf melt rate that are more than 10 m·yr^{-1}. Our work confirms previous findings (Alley et al., 2016; Le Brocq et al., 2013) showing subglacial discharge outlet locations line up well with surface channels visible in the MODIS-based Mosaic of Antarctica (MOA) image (Scambos et al., 2007)(see Supplementary Fig. ~~S6~~S7).

4 Discussion

4.1 The continuity of the troughs

The deep troughs we find extending from the inner continental shelf to Getz and are deep enough to allow the CDW observed along the ice shelf calving front to enter the ice shelf cavity (Fig. 2c). The continuity of the troughs between the Getz cavity and the continental shelf suggests that the glaciers feeding Getz may have flowed down the deep troughs and onto the continental

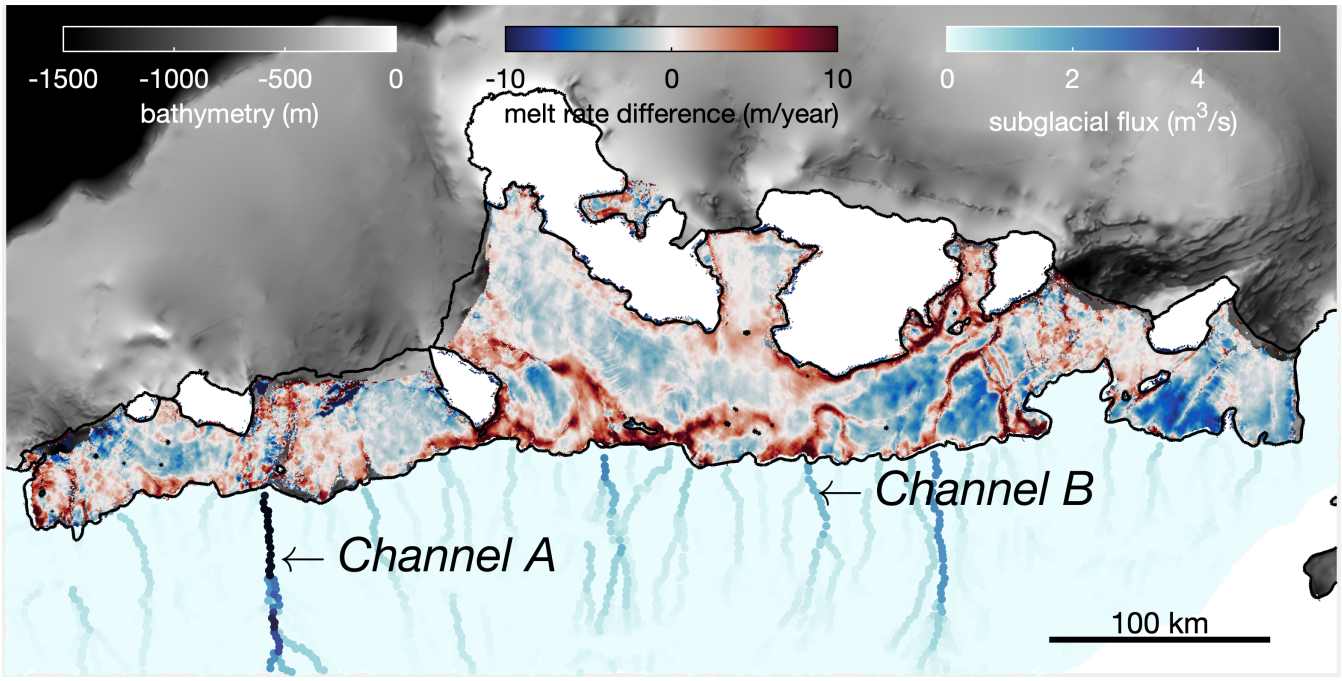

Figure 3. The melt rate difference between observed melt rate and melt rate with no discharge. Red indicates regions where observed melt rates are higher than can be explained by temperature-and-depth-dependent forcing alone. The blue fluxes indicates subglacial meltwater. The gray background is the bathymetry from IBCSO (Arndt et al., 2013).

shelf during the past ice age (Larter et al., 2009; Nitsche et al., 2007). The major troughs we report are not present in the publicly available Bedmap2 (Fretwell et al., 2013) or IBCSO (International Bathymetric Chart of the Southern Ocean) (Arndt et al., 2013) and the bathymetric sill we observe is not represented in RTOPO2 (Schaffer and Timmermann, 2016). One exception is the deep trough that is identified east of Wright Island, where the depth of trough is 200 m shallower than the trough of the inner continental shelf near the ice shelf front. This new bathymetry will provide important boundary conditions for numerical ocean modeling efforts designed to improve our understanding of ocean heat delivery to coastal ice shelves.

4.2 Impact of the ice draft on the melt rate

Previous oceanographic surveys have shown that the Getz melt rate is sensitive to ocean temperature, thermocline depth, circulation strength, bathymetry, and ice thickness (Jacobs et al., 2013). ~~We show that~~ In our study, the factors that may affect the melt rate over the trough area are bathymetry, ice bottom elevation, incursion of warm water, subglacial discharge drained across the grounding line, and the continuity of the troughs from the grounding line to the ~~pattern of basal melt is correlated with bathymetric troughs that allow CDW to access the~~ ice shelf ~~base~~ edge (Fig. 2a and 2b)~~; however, differences~~. Differences in melt regimes are apparent between the two troughs we report. Most notably, ice in the DWT experiences a much higher melt rate than ice in the SDT, likely because the deep draft of the Eastern Getz places it in warm CDW, whereas the shallow

base of the ice to the west sits in relatively cooler water. In Eastern Getz, the high basal melt region over DWT corresponds to thick ice, where the base sits in the water below the 500 -m thermocline depth (stippled region in Fig. 2b). In addition, the deep trough that is identified east of Wright Island does not correspond to a high melt rate. There is no pathway for CDW intrusion to the ice shelf cavity over that deep trough since the trough is not continuous from the inner continental shelf to the ice shelf cavity. Therefore, the deep trough that lies east of Wright Island is not associated with a major basal melting although the corresponding ice draft is deep (Fig. 2b).

The existence of a trough does not necessarily indicate that the melt rate will be high over it. XY is overlain by a deep trough and allows the incursion of CDW with high melt rate at the grounding line. However, the ice draft is shallower than the thermocline depth, so we do not observe high melt rate all along the trough overlain by XY. Similarly, the melt rate is high over DWT since the ice draft is deeper than the thermocline depth. In addition, subglacial hydrological modeling (Figure 3) suggests that the subglacial meltwater from upstream may drain through channel B and enhance the melt rate near Y. Therefore, although Y has a relatively shallow bathymetry, we observe a melt rate peak around Y.

4.3 Impact of the subglacial discharge on the melt rate

The map of basal melt rate shows several areas of localized high values along channel-like structures connected to the grounding lines. Analysis of subglacial discharge shows a striking connection between predicted channel outlets and high basal melt rates, suggesting that subglacial discharge plays a significant role in regulating the basal melt rate in Getz. Several of the channel outlet locations predicted by GlaDS correspond to ice shelf melt rates that are more than 10 $\mathrm{m \cdot yr^{-1}}$ higher than can be explained by thermal ocean forcing alone (Fig. 3).

Subglacial discharge has been shown to increase basal melt by initiating convective cells carrying heat from warm ocean water below the thermocline to the underside of ice shelves and calving fronts (Jenkins, 2011; Slater et al., 2015). This correspondence is because the subglacial meltwater from upstream drains across the grounding line and induces large but localized sub-ice-shelf melt rates beneath the ice shelf (Le Brocq et al., 2013). One notable exception is Channel A, which pumps more subglacial discharge into the cavity than any other source, yet ice shelf melt rates here are not anomalously high. This is likely due to the presence of a bathymetric high (Fig. 2a) that prevents CDW from entering the Getz cavity to the west of Dean Island. As a result, buoyant subglacial discharge from Channel A does not entrain warm water into its plume or cause elevated channelized melt rates west of Dean Island.

5 Conclusions

Our new bathymetry of the Getz Ice Shelf reveals troughs that are continuous from the inner continental shelf to the ice sheet grounding line, which provide natural pathways for CDW to enter into the ice cavity and drive rapid basal melt. We show discharge of subglacial freshwater plays a significant role in regulating the basal melt rate of Getz. Our results confirm the importance of bathymetry and subglacial discharge for understanding ocean forcing on basal mass loss of Antarctic ice shelves. Our study demonstrates the practical use of high-resolution ship-borne helicopter gravity to fill critical gaps in seafloor

bathymetry in Antarctica, especially over the deep troughs under the ice-shelf cavity that generally go undetected in more regional aerogeophysical surveys. These new data will be critical for guiding new airborne/ground-based surveys, interpreting recent and past ice-shelf changes, and informing ocean circulation modeling of future impacts for this sector of West Antarctica. The controls from bathymetry and subglacial discharge on the ice shelf basal melting we have found here is likely widespread around Antarctica. Therefore, a similar study over other massive ice shelves ~~such as~~ similar to Getz should be addressed in the future~~study~~.

Data availability. The IceBridge gravity and radar data were obtained from https://nsidc.org/icebridge/portal/. Helicopter gravity data will be deposited at https://gcmd.nasa.gov/. The CTD casts were obtained from https://www.nodc.noaa.gov/OC5/woa13/. The CryoSat-2 satellite altimetry data are available at https://earth.esa.int/web/guest/data-access. The ice velocity data were obtained from https://nsidc.org/data/nsidc-0484/. The derived data products in this paper is posted at https://doi.org/10.5281/zenodo.2527237.

Author contributions. W.W. performed the gravity inversion and wrote the manuscript; J.S.G assisted with mapping and gravity inversion processing; N.G performed the observed melt rate calculation; C.F.G. conducted the hydrological model study; C.A.G. estimated non-discharge case melt rate and assisted with Antarctic Mapping Tool; D.D.B. and D.A.Y. supported with the geophysical interpretations; A.W., and K.A. contributed the oceanographic inputs; T.G.R., S.H.L., T.W.K. and W.S.L. contributed to the helicopter gravity data collection. All authors contributed comments to the interpretation of results and preparation of the final paper.

Competing interests. The authors declare that they have no competing financial interests.

Acknowledgements. This work was supported by the NSF project (grant PLR-1543452), G. Vetlesen Foundation, and UTIG Gale White Fellowship. The non-discharge case melt rate research was carried out at the Jet Propulsion Laboratory, California Institute of Technology, under a contract with the National Aeronautics and Space Administration. Work on the observed melt rate was funded by European Space Agency's Support to Science Element programme through CryoTop Evolution project 4000116874/16/I-NB (NG). We thank KOPRI and Helicopter New Zealand for collecting the helicopter gravity data across the Amundsen Sea Sector. Helicopter gravity survey is supported by the Korean Ministry of Oceans and Fisheries (KIMST20190361; PM19020) and KOPRI PE18060. We also thank Geosoft Education Program for sponsoring the software to conduct the bathymetry inversion. This is UTIG contribution ####.

References

Alley, K. E., Scambos, T. A., Siegfried, M. R., and Fricker, H. A.: Impacts of warm water on Antarctic ice shelf stability through basal channel formation, Nature Geoscience, 9, 290–293, https://doi.org/10.1038/ngeo2675, 2016.

Arndt, J., Schenke, H., Jakobsson, M., Nitsche, F. O., Buys, G., Goleby, B., Rebesco, M., Bohoyo, F., Hong, J., and Black, J.: The International Bathymetric Chart of the Southern Ocean (IBCSO) Version 1.0–A new bathymetric compilation covering circum Antarctic waters, Geophysical Research Letters, 40, 3111–3117, https://doi.org/10.1002/grl.50413, 2013.

Assmann, K., Darelius, E., Wåhlin, A., Kim, T., and Lee, S.: Warm Circumpolar Deep Water at the Western Getz Ice Shelf Front, Antarctica, Geophysical Research Letters, https://doi.org/10.1029/2018gl081354, 2019.

Briggs, I. C.: Machine contouring using minimum curvature, Geophysics, 39, 39–48, 1974.

Cochran, J. and Bell, R.: IceBridge Sander AIRGrav L1B Geolocated Free Air Gravity Anomalies, Version 1 [updated 2018], Boulder, Colorado USA. NASA National Snow and Ice Data Center Distributed Active Archive Center, https://doi.org/https://doi.org/10.5067/R1RQ6NRIJV89, 2010.

Cochran, J., Jacobs, S., Tinto, K., and Bell, R.: Bathymetric and oceanic controls on Abbot Ice Shelf thickness and stability, The Cryosphere, 8, 877–889, https://doi.org/10.5194/tc-8-877-2014, 2014.

Cochran, J. R. and Bell, R. E.: Inversion of IceBridge gravity data for continental shelf bathymetry beneath the Larsen Ice Shelf, Antarctica, Journal of Glaciology, 58, 540–552, https://doi.org/10.3189/2012JoG11J033, 2012.

Dow, C. F., Werder, M. A., Nowicki, S., and Walker, R. T.: Modeling Antarctic subglacial lake filling and drainage cycles, The Cryosphere, 10, 1381–1393, 2016.

Dow, C. F., Werder, M. A., Babonis, G., Nowicki, S., Walker, R. T., Csathó, B., and Morlighem, M.: Dynamics of active subglacial lakes in Recovery Ice Stream, Journal of Geophysical Research: Earth Surface, 123, 837–850, 2018.

Dow, C. S., McCormack, F. S., Young, D. A., Greenbaum, J. S., Roberts, J. L., and Blankenship, D. D.: Totten Glacier subglacial hydrology determined from geophysics and modeling, Earth and Planetary Science Letters, submitted.

Förste, C., Schmidt, R., Stubenvoll, R., Flechtner, F., Meyer, U., König, R., Neumayer, H., Biancale, R., Lemoine, J.-M., Bruinsma, S., et al.: The GeoForschungsZentrum Potsdam/Groupe de Recherche de Geodesie Spatiale satellite-only and combined gravity field models: EIGEN-GL04S1 and EIGEN-GL04C, Journal of Geodesy, 82, 331–346, 2008.

Fretwell, P., Pritchard, H., Vaughan, D., Bamber, J., Barrand, N., Bell, R., Bianchi, C., Bingham, R., Blankenship, D., Casassa, G., Catania, G., Callens, D., Conway, H., Cook, A., Corr, H., Damaske, D., Damm, V., Ferraccioli, F., Forsberg, R., Fujita, S., Gim, Y., Gogineni, P., Griggs, J., Hindmarsh, R., Holmlund, P., Holt, J., Jacobel, R., Jenkins, A., Jokat, W., Jordan, T., King, E., Kohler, J., Krabill, W., M., R., Langley, K., Leitchenkov, G., Leuschen, C., Luyendyk, B., Matsuoka, K., Mouginot, J., Nitsche, F., Nogi, Y., Nost, O., Popov, S., Rignot, E., Rippin, D., Rivera, A., Roberts, J., Ross, N., Siegert, M., Smith, A., Steinhage, D., Studinger, M., Sun, B., Tinto, B., Welch, B., Wilson, D., Young, D., Xiangbin, C., and Zirizzotti, A.: Bedmap2: improved ice bed, surface and thickness datasets for Antarctica, The Cryosphere, 7, 375–393, https://doi.org/10.5194/tc-7-375-2013, 2013.

Gohl, K., Denk, A., Eagles, G., and Wobbe, F.: Deciphering tectonic phases of the Amundsen Sea Embayment shelf, West Antarctica, from a magnetic anomaly grid, Tectonophysics, 585, 113–123, 2013.

Gourmelen, N., Escorihuela, M., Shepherd, A., Foresta, L., Muir, A., Garcia-Mondejar, A., Roca, M., Baker, S., and Drinkwater, M.: CryoSat-2 swath interferometric altimetry for mapping ice elevation and elevation change, Advances in Space Research, 2017a.

Gourmelen, N., Goldberg, D., Snow, K., Henley, S., Bingham, R., Kimura, S., Hogg, A., Shepherd, A., Mouginot, J., Lenaerts, J., Ligtenberg, S., and Berg, W.: Channelized melting drives thinning under a rapidly melting Antarctic ice shelf, Geophysical Research Letters, 44, 9796–9804, https://doi.org/10.1002/2017GL074929, 2017b.

Greenbaum, J., Blankenship, D., Young, D., Richter, T., Roberts, J., Aitken, A., Legresy, B., Schroeder, D., Warner, R., Ommen, T., and Siegert, M.: Ocean access to a cavity beneath Totten Glacier in East Antarctica, Nature Geoscience, 8, 294–298, https://doi.org/10.1038/ngeo2388, 2015.

Greene, C. A., Gwyther, D. E., and Blankenship, D. D.: Antarctic Mapping Tools for MATLAB, Computers & Geosciences, 104, 151–157, https://doi.org/10.1016/j.cageo.2016.08.003, 2017.

Greene, C. A., Thirumalai, K., Kearney, K. A., Delgado, J., Schwanghart, W., Wolfenbarger, N. S., Thyng, K. M., Gwyther, D. E., Gardner, A. S., and Blankenship, D. D.: The Climate Data Toolbox for MATLAB, Geochem Geophys Geosystems, https://doi.org/10.1029/2019gc008392, 2019.

Gwyther, D. E., Galton-Fenzi, B. K., Dinniman, M. S., Roberts, J. L., and Hunter, J. R.: The effect of basal friction on melting and freezing in ice shelf–ocean models, Ocean Modelling, 95, 38–52, 2015.

Holland, P. R., Jenkins, A., and Holland, D. M.: The response of ice shelf basal melting to variations in ocean temperature, Journal of Climate, 21, 2558–2572, 2008.

Howat, I. M., Porter, C., Smith, B. E., Noh, M.-J., and Morin, P.: The Reference Elevation Model of Antarctica, The Cryosphere, 13, 665–674, 2019.

Jacobs, S., Giulivi, C., Dutrieux, P., Rignot, E., Nitsche, F., and Mouginot, J.: Getz Ice Shelf melting response to changes in ocean forcing, Journal of Geophysical Research: Oceans, 118, 4152–4168, https://doi.org/10.1002/jgrc.20298, 2013.

Jenkins, A.: A one-dimensional model of ice shelf-ocean interaction, Journal of Geophysical Research: Oceans, 96, 20 671–20 677, 1991.

Jenkins, A.: Convection-driven melting near the grounding lines of ice shelves and tidewater glaciers, Journal of Physical Oceanography, 41, 2279–2294, 2011.

Jourdain, N. C., Mathiot, P., Merino, N., Durand, G., Le Sommer, J., Spence, P., Dutrieux, P., and Madec, G.: Ocean circulation and sea-ice thinning induced by melting ice shelves in the Amundsen Sea, Journal of Geophysical Research: Oceans, 122, 2550–2573, 2017.

Larter, R. D., Graham, A. G., Gohl, K., Kuhn, G., Hillenbrand, C.-D., Smith, J. A., Deen, T. J., Livermore, R. A., and Schenke, H.-W.: Subglacial bedforms reveal complex basal regime in a zone of paleo–ice stream convergence, Amundsen Sea Embayment, West Antarctica, Geology, 37, 411–414, 2009.

Le Brocq, A. M., Ross, N., Griggs, J. A., Bingham, R. G., Corr, H. F., Ferraccioli, F., Jenkins, A., Jordan, T. A., Payne, A. J., Rippin, D. M., and Siegert, M. J.: Evidence from ice shelves for channelized meltwater flow beneath the Antarctic Ice Sheet, Nature Geoscience, 6, 945–948, https://doi.org/10.1038/ngeo1977, 2013.

Ligtenberg, S., Helsen, M., and Van den Broeke, M.: An improved semi-empirical model for the densification of Antarctic firn, The Cryosphere, 5, 809–819, 2011.

Little, C. M., Gnanadesikan, A., and Oppenheimer, M.: How ice shelf morphology controls basal melting, Journal of Geophysical . . . , 114, https://doi.org/10.1029/2008jc005197, 2009.

Locarnini, R., Mishonov, A., Antonov, J., Boyer, T., Garcia, H., Baranova, O., Zweng, M., Paver, C., Reagan, J., and Johnson, D.: World Ocean Atlas 2013, Volume 1: Temperature, edited by: Levitus, S, A. Mishonov Technical Ed.; NOAA Atlas NESDIS, 73, 40 pp, 2013.

Marsh, O. J., Fricker, H. A., Siegfried, M. R., Christianson, K., Nicholls, K. W., Corr, H. F., and Catania, G.: High basal melting forming a channel at the grounding line of Ross Ice Shelf, Antarctica, Geophysical Research Letters, 43, 250–255, https://doi.org/10.1002/2015gl066612, 2016.

McDougall, T. and Barker, P.: Getting started with TEOS-10 and the Gibbs Seawater (GSW) Oceanographic Toolbox, SCOR/IAPSO WG127, 2011.

Millan, R., Rignot, E., Bernier, V., Morlighem, M., and Dutrieux, P.: Bathymetry of the Amundsen Sea Embayment sector of West Antarctica from Operation IceBridge gravity and other data, Geophysical Research Letters, 44, 1360–1368, https://doi.org/10.1002/2016GL072071, 2017.

Mouginot, B., Scheuchl, J., and Rignot, E.: MEaSUREs Antarctic boundaries for IPY 2007–2009 from satellite radar, version 2, Boulder, CO: NASA National Snow and Ice Data Center Distributed Active Archive Center. https://doi. org/10.5067/AXE4121732AD, 2017.

Mukasa, S. B. and Dalziel, I. W.: Marie Byrd Land, West Antarctica: Evolution of Gondwana's Pacific margin constrained by zircon U-Pb geochronology and feldspar common-Pb isotopic compositions, Geological Society of America Bulletin, 112, 611–627, https://doi.org/10.1130/0016-7606(2000)112<611:MBLWAE>2.0.CO;2, 2000.

Muto, A., Peters, L. E., Gohl, K., Sasgen, I., Alley, R. B., Anandakrishnan, S., and Riverman, K. L.: Subglacial bathymetry and sediment distribution beneath Pine Island Glacier ice shelf modeled using aerogravity and in situ geophysical data: New results, Earth and Planetary Science Letters, 433, 63–75, 2016.

Nakayama, Y., Timmermann, R., Rodehacke, C. B., Schröder, M., and Hellmer, H. H.: Modeling the spreading of glacial meltwater from the Amundsen and Bellingshausen Seas, Geophysical Research Letters, 41, 7942–7949, 2014.

Nitsche, F., Jacobs, S., Larter, R., and Gohl, K.: Bathymetry of the Amundsen Sea continental shelf: Implications for geology, oceanography, and glaciology, Geochemistry, Geophysics, Geosystems, 8, https://doi.org/10.1029/2007GC001694, 2007.

Paolo, F. S., Fricker, H. A., and Padman, L.: Volume loss from Antarctic ice shelves is accelerating, Science, 348, 327–331, https://doi.org/10.1126/science.aaa0940, 2015.

Pattyn, F.: Antarctic subglacial conditions inferred from a hybrid ice sheet/ice stream model, Earth and Planetary Science Letters, 295, 451–461, 2010.

Raiswell, R., Tranter, M., Benning, L. G., Siegert, M., De'ath, R., Huybrechts, P., and Payne, T.: Contributions from glacially derived sediment to the global iron (oxyhydr) oxide cycle: implications for iron delivery to the oceans, Geochimica et Cosmochimica Acta, 70, 2765–2780, https://doi.org/10.1016/j.gca.2005.12.027, 2006.

Rignot, E., Jacobs, S., Mouginot, J., and Scheuchl, B.: Ice-shelf melting around Antarctica, Science, 341, 266–270, https://doi.org/10.1126/science.1235798, 2013.

Rignot, E., Mouginot, J., and Scheuchl, B.: MEaSUREs InSAR-based Antarctica ice velocity map, Version 2. Boulder, Colorado USA. NASA National Snow and Ice Data Center Distributed Active Archive Center, 2017.

Scambos, T., Haran, T., Fahnestock, M., Painter, T., and Bohlander, J.: MODIS-based Mosaic of Antarctica (MOA) data sets: Continent-wide surface morphology and snow grain size, Remote Sensing of Environment, 111, 242–257, 2007.

Schaffer, J. and Timmermann, R.: Greenland and Antarctic ice sheet topography, cavity geometry, and global bathymetry (RTopo-2), links to NetCDF files, https://doi.org/10.1594/PANGAEA.856844, https://doi.org/10.1594/PANGAEA.856844, supplement to: Schaffer, Janin; Timmermann, Ralph; Arndt, Jan Erik; Kristensen, Steen Savstrup; Mayer, Christoph; Morlighem, Mathieu; Steinhage, Daniel (2016): A global, high-resolution data set of ice sheet topography, cavity geometry, and ocean bathymetry. Earth System Science Data, 8(2), 543-557, https://doi.org/10.5194/essd-8-543-2016, 2016.

Silvano, A., Rintoul, S. R., Peña-Molino, B., Hobbs, W. R., van Wijk, E., Aoki, S., Tamura, T., and Williams, G. D.: Freshening by glacial meltwater enhances melting of ice shelves and reduces formation of Antarctic Bottom Water, Science advances, 4, eaap9467, 2018.

Slater, D., Nienow, P., Cowton, T., Goldberg, D., and Sole, A.: Effect of near terminus subglacial hydrology on tidewater glacier submarine melt rates, Geophysical Research Letters, 42, 2861–2868, https://doi.org/10.1002/2014GL062494, 2015.

Talwani, M., Worzel, L. J., and Landisman, M.: Rapid gravity computations for two–dimensional bodies with application to the Mendocino submarine fracture zone, Journal of Geophysical Research, 64, 49–59, https://doi.org/10.1029/jz064i001p00049, 1959.

Tinto, K. and Bell, R.: Progressive unpinning of Thwaites Glacier from newly identified offshore ridge: Constraints from aerogravity, Geophysical Research Letters, 38, https://doi.org/10.1029/2011GL049026, 2011.

Van Wessem, J., Ligtenberg, S., Reijmer, C., Van De Berg, W., Van Den Broeke, M., Barrand, N., Thomas, E., Turner, J., Wuite, J., Scambos, T., and Van Meijgaard, E.: The modelled surface mass balance of the Antarctic Peninsula at 5.5 km horizontal resolution, The Cryosphere, 10, 271–285, 2016.

Werder, M. A., Hewitt, I. J., Schoof, C. G., and Flowers, G. E.: Modeling channelized and distributed subglacial drainage in two dimensions, Journal of Geophysical Research: Earth Surface, 118, 2140–2158, https://doi.org/10.1002/jgrf.20146, 2013.